Satellite-derived precipitation data calibration using ground-based rain gauge observations by means of machine learning methods

Navid Bagherpour[a], Mohammad Reza Saradjian[b*]

[a,b]School of Surveying and Geospatial Engineering, College of Engineering, University of Tehran, Tehran, Iran

* Corresponding author

Keywords: Precipitation, Bias Correction, Machine learning, Regression, Remote Sensing

Abstract

Accurate precipitation estimation is vital for water resource management, climate monitoring, and natural hazard assessment. However, satellite precipitation products (SPPs) such as CHIRPS and GPM often exhibit significant biases, particularly over complex mountainous regions. This study aims to improve precipitation estimates across Mazandaran Province, northern Iran, by integrating satellite data with rain gauge observations through machine learning (ML) approaches. Monthly precipitation records from 190 stations (2000–2024) were combined with SPPs and environmental predictors, including elevation, soil moisture, temperature, and land cover. Two ML models—Extreme Gradient Boosting (XGBoost) and Multi-Layer Perceptron (MLP)—were implemented to correct satellite biases and enhance spatial precipitation accuracy. Both models substantially reduced estimation errors relative to raw satellite data, with XGBoost achieving superior performance. The mean RMSE decreased by approximately 20–30 mm, and correlation coefficients increased from about 0.4–0.5 to 0.6. Feature importance analysis indicated that GPM, CHIRPS, and elevation were the most influential predictors. Stratified evaluation by elevation, rainfall intensity, and forest cover revealed that XGBoost maintained robust performance under diverse environmental conditions, while MLP was more sensitive to topographic variability. Overall, the integration of multi-source data and ML-based bias correction demonstrates strong potential for improving precipitation accuracy in regions with complex topography and sparse gauge coverage, supporting more reliable hydrological and climate applications.

1. INTRODUCTION

Precipitation is one of the key hydrometeorological variables that plays a pivotal role in the global water cycle (Xiao et al., 2022). Accurate precipitation data are critical for numerous applications, including climate studies, water resource management, natural disaster forecasting, and agricultural planning, as these data can enhance economic and social planning (Kimani et al., 2018; Zhou et al., 2022). However, precipitation exhibits significant spatial and temporal variability due to complex interactions between mid-scale atmospheric systems and local conditions such as topography. To mitigate risks associated with water-related hazards, accurate estimation of regional precipitation characteristics is essential (Kumar et al., 2019; Yoshikane and Yoshimura, 2022).

Common methods for measuring precipitation include ground-based rain gauges, weather radars, and satellite observations (Lober et al., 2023; Wehbe et al., 2020). Ground-based rain gauges provide the most reliable point-based measurements (Iqbal et al., 2022; Le et al., 2023), but their spatial coverage, particularly in semi-arid or mountainous regions, is limited due to factors such as high altitudes, complicated topography, isolated locations, and insufficient funding (Le et al., 2023). These instruments may be affected by systematic and random errors caused by factors such as wind, evaporation, splashing, and snow drift (Cheema and Bastiaanssen, 2012), and these uncertainties increase when scaling point measurements to larger spatial domains (Yang et al., 2016). Despite these limitations, ground-based rain gauge data are widely accepted as a reliable source for measuring precipitation at specific points (Kimani et al., 2018; Zhou et al., 2022). Weather radars offer broader spatial coverage but measure precipitation indirectly and are constrained by specific ranges and line-of-sight limitations (Lober et al., 2023).

Satellite-based precipitation products (SPPs) serve as an alternative for regions with limited or unavailable ground-based data (Yang et al., 2016) and provide high spatial and temporal coverage (Wehbe et al., 2020). Notable examples of these products include data from the TRMM mission and its successor GPM, as well as CMORPH, PERSIANN, and CHIRPS (Lu et al., 2018; Wehbe et al., 2020). SPPs often exhibit significant discrepancies with ground-based data, necessitating error and bias reduction to improve the representation of local precipitation variations (Kimani et al., 2018). Studies have shown that these products suffer from systematic errors that lead to underestimation or overestimation of precipitation. These errors are inherently caused by retrieval algorithms, indirect measurements, and sensor limitations (Lober et al., 2023; Zhang et al., 2021). For instance, SPPs primarily rely on passive microwave reflections and infrared radiation (Iqbal et al., 2022), but infrared sensors may erroneously detect non-precipitating cold clouds as precipitation, while passive microwave sensors often underestimate intense local precipitation (Zhang et al., 2021). Additionally, several factors such as topography, geographical location, climate, season, and precipitation intensity can further complicate the errors in SPPs (Kumar et al., 2019; Lober et al., 2023). Previous studies have indicated that the performance of these products decreases with increasing elevation and is influenced by wind direction and steep slopes. Complex topography and steep slopes also contribute to increased errors (Lober et al., 2023).

Therefore, biases in SPPs represent a significant challenge that requires correction before their use in hydrometeorological research (Meema et al., 2025). Such corrections can substantially enhance the accuracy and applicability of these products in hydrological modeling (Le et al., 2023). In recent years, numerous efforts have been made to integrate satellite and ground-based data to improve the accuracy and spatial coverage of precipita-

tion estimates. Various methods for bias correction and data integration have been developed, which can be categorized as follows: (i) Simple statistical methods: Including inverse variance weighted averaging (Mastrantonas et al., 2019), and linear scaling (Hashemi et al., 2017), (ii) Statistical methods based on distribution or residuals: Such as kernel smoothing (Li and Shao, 2010), nonparametric quantile mapping (Katiraie-Boroujerdy et al., 2020), cumulative distribution function matching and bias ratio correction (Mastrantonas et al., 2019), (iii) Geostatistical methods: Such as geographically weighted regression (GWR) (Chao et al., 2018) and optimal interpolation (Nie et al., 2015), (iv) Advanced model-based methods: Including CoKriging (Yan et al., 2021), Censored Shifted Mixture Method (Ma et al., 2019), and Bayesian bias algorithm (Kimani et al., 2018). Although these methods are effective, many rely on stringent assumptions that may not hold in reality. Furthermore, most of these methods are designed to integrate a single satellite product with ground-based data, whereas each satellite product has its own strengths and weaknesses, and their performance varies across different regions and temporal scales. Integrating multiple satellite products could significantly improve the accuracy of estimates (Zhang et al., 2021).

In recent years, machine learning (ML) algorithms have gained increasing popularity in hydrology and climatology due to their ability to model complex and nonlinear relationships, lack of reliance on strict assumptions, flexibility in utilizing auxiliary variables, capability to integrate multiple satellite products with ground-based data, and ease of implementation. Numerous studies have employed models such as Neural Networks (NN), Random Forests (RF) and Support Vector Machines (SVM). For example, (Pratama et al., 2018) applied a genetic algorithm combined with nonlinear power transformation to correct biases in CHIRPS data. (Kumar et al., 2019) integrated near-real-time satellite precipitation data with soil moisture data and used nonlinear support vector regression to reduce biases. (Bhuiyan et al., 2020) utilized random forest and neural network models to correct errors in the GPM IMERG product in the Brahmaputra River basin. (Zarei et al., 2021) employed the Random Forest algorithm to correct biases in global cumulative precipitation forecasts from six numerical prediction models. (Zhang et al., 2021) proposed a novel double machine learning (DML) approach combining classification and regression models of RF, Artificial Neural Network (ANN), SVM, and Extreme Learning Machine (ELM) to merge multiple satellite precipitation products and gauge observations over the Chinese mainland. (Seo and Ahn, 2023) applied the LSTM model with atmospheric variables derived from WRF to correct biases in daily summer precipitation. (Meema et al., 2025) combined the ELM with a zoning approach to correct biases in APHRODITE gridded precipitation data in data-scarce regions, improving precipitation accuracy and hydrological simulation. These studies demonstrate the high potential of machine learning in enhancing precipitation estimates. Machine learning approaches offer significant advantages over traditional methods, including the ability to model nonlinear and complex relationships without requiring restrictive assumptions, flexibility in utilizing diverse data and auxiliary variables, and effective integration of multiple satellite and ground-based data sources. These features make machine learning a powerful tool for improving the accuracy of precipitation estimates and providing sustainable and efficient solutions for hydrological and climatic applications (Zhang et al., 2021).

This study aims to enhance the accuracy of precipitation estimates by exploring and developing novel methods for bias correction in satellite precipitation products (SPPs) and improving their performance in practical applications, with an emphasis on the importance of integrating ground-based and satellite data using machine learning techniques. To this end, we have utilized data from two satellite precipitation products, namely CHIRPS and GPM, along with machine learning models XGBoost and neural networks (NN) to improve precipitation estimates and correct biases. This approach is designed to leverage the strengths of both satellite products and combine them with ground-based data to provide more accurate precipitation estimates.

The structure of this paper is organized as follows: Section 2 details the materials and methodology, describing the datasets, tools, and techniques employed in this study. Section 3 presents the results, analyzing the performance of the proposed methods. Finally, Section 4 discusses the findings, their implications, and potential avenues for future research.

2. MATERIALS AND METHODS

2.1 Study area

The study area is Mazandaran Province, located in northern Iran (Figure 1). The province covers an area of approximately 23,833 km^2, situated between latitudes 35.75°N and 37.00°N, and longitudes 50.3°E to 54.16°E. Mazandaran is bounded by the Caspian Sea to the north and the Alborz mountain range to the south.

The topography of the province is diverse, with mountainous terrain in the south and west, and coastal plains in the northeastern part, resulting in an elevation difference of about 5,500 meters across the region. Climatically, Mazandaran exhibits a humid and semi-tropical climate in the coastal areas and a temperate to cold climate in the mountainous zones. The influence of the Caspian Sea and the province's complex topography contribute to significant precipitation throughout the year, which is relatively evenly distributed across seasons but peaks during autumn and winter. The average annual precipitation is approximately 600 mm. High humidity levels have led to the growth of dense forests, covering around 41% of the province's area.

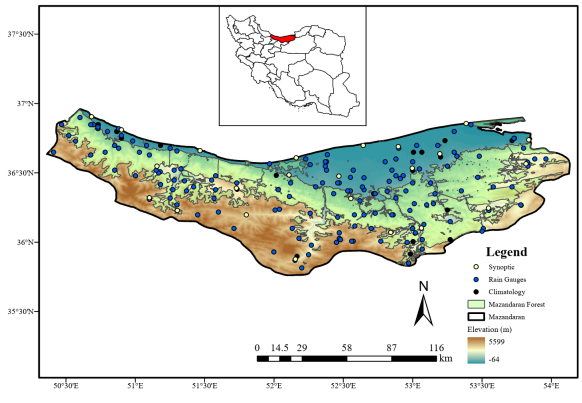

Figure 1. Geographic location of the study area (Mazandaran Province) in northern Iran, including the distribution of stations used in this study

2.2 Dataset

(1) Rain gauge:

The study area comprises a total of 190 meteorological stations, including 18 climatological stations, 149 rain gauge stations,

and 23 synoptic stations, which are approximately evenly distributed across the province. Monthly rainfall data from these stations, spanning the period from 2000 to 2024, were acquired from the Iran Meteorological Organization.

(2) CHIRPS:

The CHIRPS dataset has been available since 1981 with a spatial resolution of 0.05 degrees and has been released in three versions (v1.0, v2.0, and v3.0). Versions v2.0 and v3.0 incorporate more extensive station and satellite data compared to the initial release, with version v3.0 further integrating IMERG data and applying station bias corrections. In this study, monthly CHIRPS data version 3.0 spanning from 2000 to 2024 were obtained from the Climate Hazards Center (CHC).

(3) GPM IMERG

The GPM IMERG dataset, available since 2000 with a spatial resolution of 0.1 degrees, has been released in multiple versions, with the latest being v7.0. Data prior to February 2014 consist of reprocessed measurements from the TRMM mission and other satellites, processed using advanced algorithms to enhance accuracy and consistency with GPM data. Compared to earlier versions, v6.0 and v7.0 incorporate improved satellite data intercalibration and enhanced algorithms, with v7.0 further integrating advanced infrared retrievals, refined gridding processes, and additional passive microwave data for greater accuracy. In this study, monthly GPM IMERG v7.0 data spanning from 2000 to 2024 were obtained from the NASA Global Precipitation Measurement (GPM) mission archive.

(4) Environmental factors

In this study, in addition to precipitation data, the Digital Elevation Model (DEM) from the SRTM mission with a 30-meter resolution, as well as soil moisture and temperature from the ERA5-Land dataset, were utilized. The SRTM 30 data, collected in 2000 by NASA and USGS, provide detailed topographic information for elevation analyses. The ERA5-Land soil moisture and 2-meter air temperature data, with a spatial resolution of 0.1 degrees and a monthly temporal resolution, were obtained for the period 2000 to 2024 from the ECMWF. These data were generated using advanced reanalysis techniques to ensure high accuracy for hydrological and climatic analyses.

Table 1 presents the datasets used in this study.

Data	Datasets	Resolution
Precipitation	Rain gauges	Daily, Points
	CHIRPS	Daily, ∼5km
	GPM IMERG	Daily, ∼10km
DEM	SRTM	-, 30m
Soil Moisture	ERA-5 LAND	Daily, ∼10km
Temperature	ERA-5 LAND	Daily, ∼10km

Table 1. Datasets used in this study

2.3 Methodology

This study aims to analyze satellite precipitation data and correct their biases using two machine learning methods, XGBoost and MLP. The data were preprocessed, and their spatial resolution was standardized to ensure consistency across different datasets. Optimal parameters for each model were determined using Grid Search. To prevent overfitting, Early Stopping was employed. The methodology involves applying predictive models to enhance the accuracy of precipitation estimates, with details of these models described subsequently. The input data for this study comprised satellite precipitation and auxiliary variables, such as elevation, soil moisture, and 2-meter air temperature. These data were preprocessed and their spatial resolution was standardized to ensure consistency across different datasets for modeling.

2.3.1 Multi-Layer Perceptron (MLP): The MLP, a feed-forward neural network, was employed in this study to correct biases in satellite precipitation data. The model consists of two hidden layers, the first with 100 neurons and the second with 50 neurons, and utilizes the ReLU activation function to capture nonlinear patterns. The MLP was trained using the Adam optimization algorithm with an initial learning rate of 0.001 to minimize precipitation estimation errors and enhance prediction accuracy.

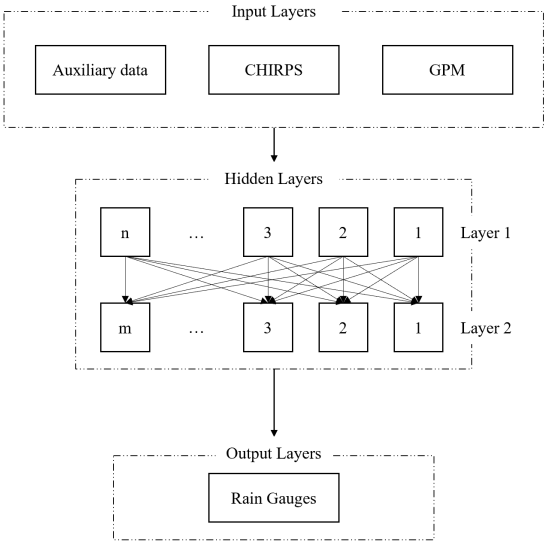

Figure 2. Flowchart for MLP model

2.3.2 Extreme Gradient Boosting (XGBoost): The XGBoost (Extreme Gradient Boosting) model, a tree-based machine learning algorithm, was employed in this study to correct biases in satellite precipitation data. The model utilizes 509 decision trees with a maximum depth of 5 and a learning rate of 0.01, trained sequentially, optimizing a gradient-based objective function to capture complex patterns. The XGBoost model was trained to minimize precipitation estimation errors and enhance prediction accuracy.

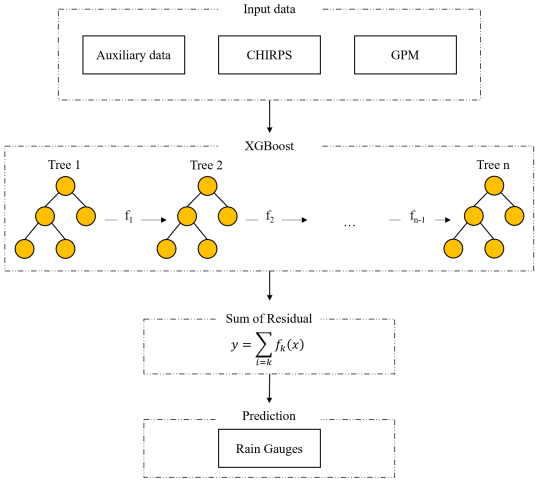

Figure 3. Flowchart for XGBoost model

This contribution has been peer-reviewed. The double-blind peer-review was conducted on the basis of the full paper.
https://doi.org/10.5194/isprs-annals-X-4-W8-2025-141-2026 | © Author(s) 2026. CC BY 4.0 License.

2.4 Accuracy Metrics

To assess the accuracy and reliability of the results obtained from this study, four accuracy metrics were used: Root Mean Square Error (RMSE), Coefficient of Determination (R^2), Mean Absolute Error (MAE), and Correlation Coefficient (CC). These metrics, by comparing the outputs of the methods with reference data, assessed their effectiveness in improving precipitation estimates and correcting biases in satellite data. The formulas for these metrics are provided below:

$$CC = \frac{\sum_{i=1}^{n}(E_i - \overline{E})(O_i - \overline{O})}{\sqrt{\sum_{i=1}^{n}(E_i - \overline{E})^2} \times \sqrt{\sum_{i=1}^{n}(O_i - \overline{O})^2}} \quad (1)$$

$$MAE = \frac{\sum_{i=1}^{n}|E_i - O_i|}{n} \quad (2)$$

$$RMSE = \sqrt{\frac{1}{n}\sum_{i=1}^{n}(E_i - O_i)^2} \quad (3)$$

$$R^2 = 1 - \frac{\sum_{i=1}^{n}(E_i - O_i)^2}{\sum_{i=1}^{n}(O_i - \overline{O})^2} \quad (4)$$

Where E_i is the satellite-based or estimated precipitation at station i, O_i is the rain gauge precipitation at station i, $\overline{E}$ and $\overline{O}$ are the mean satellite-based or estimated and rain gauge precipitation values, respectively, and n is the number of stations.

3. RESULTS

The dataset used in this study consists of a total of 30,618 samples, divided into training and testing subsets. The training set covers the period from 2000 to 2019, comprising 25,682 samples, while the testing set includes 4,936 samples from 2019 to 2024.

Input features consist of station ID, satellite-derived precipitation data from CHIRPS and GPM, month of observation, station elevation, forest/non-forest classification, soil moisture, and temperature. Ground-based station measurements were used as the target variable.

Table 2 presents a performance comparison of precipitation estimation methods on the test dataset. Evaluation metrics were calculated on the test dataset for CHIRPS and GPM satellite products, as well as for the outputs of the XGBoost and MLP models. Results indicate that machine learning models substantially improve precipitation estimation accuracy.

Dataset	RMSE (mm)	MAE (mm)	R^2	CC
CHIRPS	59.29	41.00	-0.07	0.41
GPM	72.03	48.86	-0.59	0.48
XGBoost	**45.45**	**29.79**	**0.37**	**0.61**
MLP	49.48	33.00	0.25	0.52

Table 2. Performance comparison of precipitation estimation methods on the test dataset. Note: Negative R^2 values indicate that model error exceeds the variance of observations

Specifically, for CHIRPS data, RMSE = 59.29 mm, MAE = 41 mm, R^2 = -0.07, and correlation coefficient (CC) = 0.41 were obtained. For GPM data, RMSE = 72.03 mm, MAE = 48.86 mm, R^2 = -0.59, and CC = 0.48 were observed. After applying the XGBoost model, the performance improved to RMSE = 45.45 mm, MAE = 29.79 mm, R^2 = 0.37, and CC = 0.61. The MLP model yielded RMSE = 49.48 mm, MAE = 33 mm, R^2 = 0.25, and CC = 0.52. These results demonstrate that the machine learning models reduced error by approximately 10 mm and 15 mm compared to CHIRPS data, and by approximately 23 mm and 28 mm compared to GPM data for MLP and XGBoost, respectively (Table 2). Feature importance analysis revealed that GPM data, followed by CHIRPS data and elevation, had the greatest influence on the models and contributed most to the improvements.

Dataset	RMSE	MAE	R^2	CC
Elevation: High, Rainfall: High				
CHIRPS	**64.80**	**50.08**	**-0.51**	0.36
GPM	72.37	58.19	-0.89	0.39
XGBoost	74.67	60.82	-1.01	**0.55**
MLP	85.29	71.59	-1.62	0.43
Elevation: High, Rainfall: Medium				
CHIRPS	41.55	30.62	-10.66	0.03
GPM	53.00	40.46	-17.96	0.14
XGBoost	**19.14**	**15.14**	**-1.47**	**0.15**
MLP	23.93	19.41	-2.87	0.12
Elevation: High, Rainfall: Low				
CHIRPS	49.29	37.20	-30.14	-0.09
GPM	49.66	31.36	-30.61	-0.10
XGBoost	28.01	23.33	-9.05	**-0.05**
MLP	**25.27**	**19.02**	**-7.18**	-0.10
Elevation: Medium, Rainfall: High				
CHIRPS	**55.23**	**42.43**	**-0.71**	0.31
GPM	63.83	50.29	-1.29	**0.49**
XGBoost	67.86	54.77	-1.59	0.34
MLP	69.83	60.53	-1.74	**0.49**
Elevation: Medium, Rainfall: Medium				
CHIRPS	56.10	36.93	-19.25	0.06
GPM	48.61	35.14	-14.20	0.17
XGBoost	**17.92**	**13.96**	**-1.07**	**0.25**
MLP	25.82	19.35	-3.29	0.10
Elevation: Medium, Rainfall: Low				
CHIRPS	70.58	53.56	-45.78	**-0.12**
GPM	70.88	41.18	-46.18	-0.18
XGBoost	**35.60**	27.06	**-10.90**	-0.14
MLP	37.91	**25.90**	-12.50	-0.20
Elevation: Low, Rainfall: High				
CHIRPS	**97.00**	**69.37**	**-0.34**	0.40
GPM	103.13	82.06	-0.51	0.42
XGBoost	97.67	71.78	-0.36	**0.43**
MLP	108.09	83.01	-0.66	**0.43**
Elevation: Low, Rainfall: Medium				
CHIRPS	43.71	32.07	-9.40	0.26
GPM	59.86	45.81	-18.50	**0.35**
XGBoost	31.62	21.89	-4.44	0.29
MLP	**26.34**	**19.50**	**-2.78**	0.33
Elevation: Low, Rainfall: Low				
CHIRPS	68.51	44.90	-47.51	-0.13
GPM	89.58	50.57	-81.93	**-0.11**
XGBoost	58.93	40.28	-34.89	-0.13
MLP	**53.06**	**36.97**	**-28.10**	**-0.11**

Table 3. Evaluation metrics for Forest stations by Elevation and Rainfall categories

Further evaluation was performed based on various criteria

(Tables 3 and 4). Stations were categorized into forest and non-forest groups, and further subdivided into three classes based on elevation and precipitation percentiles (Table 5). These classes correspond to low, medium, and high elevation and precipitation levels.

Dataset	RMSE	MAE	R^2	CC
Elevation: High, Rainfall: High				
CHIRPS	74.51	56.32	-1.57	0.11
GPM	77.16	58.29	-1.76	0.15
XGBoost	**66.05**	**52.20**	**-1.02**	**0.43**
MLP	75.30	58.90	-1.63	0.14
Elevation: High, Rainfall: Medium				
CHIRPS	57.54	39.34	-23.53	0.18
GPM	58.27	44.35	-24.16	0.21
XGBoost	**16.73**	**12.93**	**-1.07**	**0.25**
MLP	19.17	14.91	-1.72	0.22
Elevation: High, Rainfall: Low				
CHIRPS	57.18	41.20	-97.89	-0.01
GPM	53.80	36.02	-86.54	**0.09**
XGBoost	**24.22**	**19.18**	**-16.75**	**0.09**
MLP	25.24	20.73	-18.27	**0.09**
Elevation: Medium, Rainfall: High				
CHIRPS	52.98	41.48	-0.76	0.37
GPM	70.34	53.10	-2.09	0.39
XGBoost	**48.00**	**37.03**	**-0.44**	**0.54**
MLP	52.64	42.00	-0.73	0.48
Elevation: Medium, Rainfall: Medium				
CHIRPS	34.11	23.05	-7.62	0.26
GPM	52.11	35.65	-19.12	0.35
XGBoost	**18.76**	13.25	**-1.61**	**0.38**
MLP	19.14	**12.72**	-1.72	0.34
Elevation: Medium, Rainfall: Low				
CHIRPS	55.51	36.77	-91.36	-0.24
GPM	83.90	46.97	-210.00	-0.24
XGBoost	**39.09**	**27.47**	**-44.81**	**-0.18**
MLP	41.86	29.64	-51.53	-0.24
Elevation: Low, Rainfall: High				
CHIRPS	72.49	52.40	-0.42	0.32
GPM	82.06	65.25	-0.81	0.51
XGBoost	**53.66**	**38.88**	**0.22**	**0.64**
MLP	58.67	41.95	0.07	0.54
Elevation: Low, Rainfall: Medium				
CHIRPS	28.34	21.15	-5.33	0.24
GPM	54.92	40.25	-22.77	**0.34**
XGBoost	**25.97**	**15.58**	**-4.31**	0.28
MLP	27.16	18.75	-4.81	0.27
Elevation: Low, Rainfall: Low				
CHIRPS	61.58	41.29	-116.51	-0.37
GPM	103.05	56.81	-328.11	**-0.25**
XGBoost	**52.92**	**33.86**	**-85.78**	-0.34
MLP	57.19	41.35	-100.35	-0.26

Table 4. Evaluation metrics for Non-Forest stations by Elevation and Rainfall categories

For non-forest stations, XGBoost generally outperformed MLP. However, in forested stations, the performance was more variable, and in some cases, the models increased errors. Under high precipitation, RMSE typically increased, but CC and R^2 also improved, indicating better model performance. Both models performed similarly in these cases, with XGBoost showing slightly better results. Under low precipitation conditions, the trend reversed: RMSE decreased while CC also declined. For medium precipitation levels, both models succeeded in reducing RMSE while maintaining or improving CC.
Regarding elevation, the models exhibited similar performance for both forest and non-forest stations when precipitation was not high. Notably, for non-forest stations at low and medium elevations, the models reduced RMSE and increased CC even under high precipitation. Additionally, XGBoost demonstrated robust performance in non-forest stations with high elevation and precipitation by reducing RMSE and increasing CC, whereas MLP was less effective. Neither model performed well for forest stations under conditions of high elevation and precipitation; notably, MLP showed a significant increase in RMSE. However, both models managed to improve CC in these situations.

Variable	Low	Medium	High
Non-Forest			
Elevation (m)	<97	97–1430	>1430
Rainfall (mm)	<17.86	17.86–57.50	>57.50
Forest			
Elevation (m)	<394	394–738	>738
Rainfall (mm)	<29.50	29.50–76.50	>76.50

Table 5. Thresholds for Elevation and Rainfall by Forest and Non-Forest groups

4. DISCUSSION

This research demonstrates the efficacy of machine learning-based bias correction techniques, specifically XGBoost and MLP, in improving the accuracy of satellite-derived precipitation data. Both models successfully reduced RMSE and enhanced correlation coefficients across various precipitation conditions, with XGBoost outperforming MLP in high precipitation scenarios. However, challenges remain in high-elevation and medium precipitation conditions, where MLP showed increased RMSE. MLP showed weaker performance in high-elevation and forested areas, likely due to complex nonlinear relationships between precipitation and environmental variables. In contrast, XGBoost effectively captured these nonlinear patterns and maintained robust performance across different elevations and land cover types. The integration of satellite data with soil moisture and elevation information proved effective in addressing spatial and temporal variability.Figure 4 presents scatterplots for XGBoost and MLP models for Train and Test data.

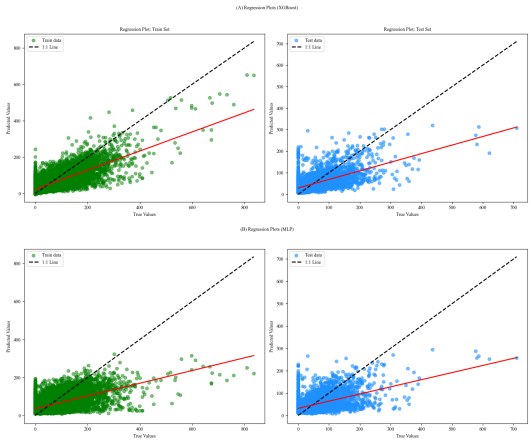

Figure 4. Scatterplots for (A) XGBoost and (B) MLP models for Train and Test

This contribution has been peer-reviewed. The double-blind peer-review was conducted on the basis of the full paper.
https://doi.org/10.5194/isprs-annals-X-4-W8-2025-141-2026 | © Author(s) 2026. CC BY 4.0 License.

The analysis of temporal and spatial precipitation patterns, as illustrated in Figures 5 to 7, further validates the effectiveness of the machine learning models. Figure 5 presents the monthly rainfall trends from 2019 to 2024, where predictions from both XGBoost and MLP closely align with ground-based rain gauge data, capturing complex temporal variability better than raw satellite products. Figure 6 shows the annual precipitation totals, demonstrating that the overestimation in GPM data is substantially corrected by the machine learning models, resulting in predictions that more accurately reflect observed values. Additionally, Figure 7 depicts the spatial distribution of annual rainfall over multiple years, highlighting improved consistency between machine learning model outputs and observed spatial rainfall patterns, particularly in complex mountainous terrain where satellite products typically exhibit higher errors. These findings underscore the robustness and reliability of integrating multiple satellite datasets with ground observations using advanced machine learning algorithms to enhance precipitation estimation accuracy across diverse temporal and spatial scales.

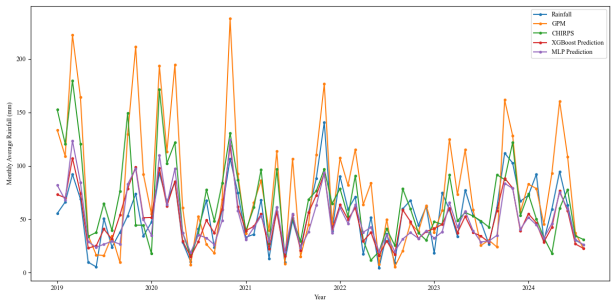

Figure 5. Monthly rainfall trends (2019–2024) comparing satellite data and ML model predictions

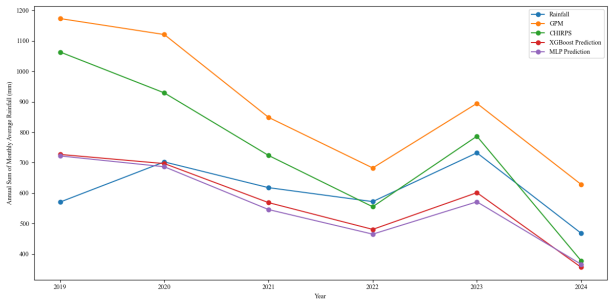

Figure 6. Annual precipitation sums (2019–2024) for satellite data and ML models

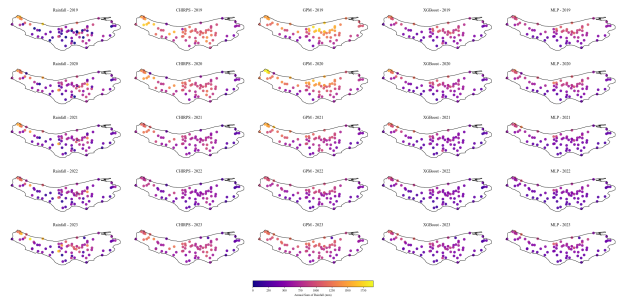

Figure 7. Spatial distribution of annual rainfall (2019–2023) across the study area

References

Bhuiyan, M., Yang, F., Biswas, N., Rahat, S., Neelam, T., 2020. Machine Learning-Based Error Modeling to Improve GPM IMERG Precipitation Product over the Brahmaputra River Basin. *Forecasting*, 2, 248–266. https://doi.org/10.3390/forecast2030014.

Chao, L., Zhang, K., Li, Z., Zhu, Y., Wang, J., Yu, Z., 2018. Geographically weighted regression based methods for merging satellite and gauge precipitation. *Journal of Hydrology*, 558, 275–289. https://doi.org/10.1016/j.jhydrol.2018.01.042.

Cheema, M., Bastiaanssen, W., 2012. Local calibration of remotely sensed rainfall from the TRMM satellite for different periods and spatial scales in the Indus Basin. *International Journal of Remote Sensing*, 33, 2603–2627. https://doi.org/10.1080/01431161.2011.617397.

Hashemi, H., Nordin, M., Lakshmi, V., Huffman, G., Knight, R., 2017. Bias Correction of Long-Term Satellite Monthly Precipitation Product (TRMM 3B43) over the Conterminous United States. *Journal of Hydrometeorology*. https://doi.org/10.1175/JHM-D-17-0025.1.

Iqbal, Z., Shahid, S., Ahmed, K., Wang, X., Ismail, T., Gabriel, H., 2022. Bias correction method of high-resolution satellite-based precipitation product for Peninsular Malaysia. *Theoretical and Applied Climatology*, 148, 1429–1446. https://doi.org/10.1007/s00704-022-04007-6.

Katiraie-Boroujerdy, P.-S., Rahnamay Naeini, M., Akbari Asanjan, A., Chavoshian, A., Hsu, K., Sorooshian, S., 2020. Bias Correction of Satellite-Based Precipitation Estimations Using Quantile Mapping Approach in Different Climate Regions of Iran. *Remote Sensing*, 12, 2102. https://doi.org/10.3390/rs12132102.

Kimani, M., Hoedjes, J., Su, Z., 2018. Bayesian Bias Correction of Satellite Rainfall Estimates for Climate Studies. *Remote Sensing*, 10, 1074. https://doi.org/10.3390/rs10071074.

Kumar, A., Ramsankaran, R., Brocca, L., Munoz-Arriola, F., 2019. A Machine Learning Approach for Improving Near-Real-Time Satellite-Based Rainfall Estimates by Integrating Soil Moisture. *Remote Sensing*, 11, 2221. https://doi.org/10.3390/rs11192221.

Le, X.-H., Nguyen Van, L., Hai Nguyen, D., Nguyen, G., Jung, S., Lee, G., 2023. Comparison of bias-corrected multisatellite precipitation products by deep learning framework. *International Journal of Applied Earth Observation and Geoinformation*, 116, 103177. https://doi.org/10.1016/j.jag.2022.103177.

Li, M., Shao, Q., 2010. An improved statistical approach to merge satellite rainfall estimates and raingauge data. *Journal of Hydrology*, 385, 51–64. https://doi.org/10.1016/j.jhydrol.2010.01.023.

Lober, C., Fayne, J., Hashemi, H., Smith, L., 2023. Bias correction of 20 years of IMERG satellite precipitation data over Canada and Alaska. *Journal of Hydrology: Regional Studies*, 47, 101386. https://doi.org/10.1016/j.ejrh.2023.101386.

Lu, X., Wei, M., Tang, G., Zhang, Y., 2018. Evaluation and correction of the TRMM 3B43V7 and GPM 3IMERGM satellite precipitation products by use of ground-based data over Xinjiang, China. *Environmental Earth Sciences*, 77, 209. https://doi.org/10.1007/s12665-018-7378-6.

Ma, Q., Xiong, L., Xia, J., Xiong, B., Yang, H., Xu, C.-Y., 2019. A Censored Shifted Mixture Distribution Mapping Method to Correct the Bias of Daily IMERG Satellite Precipitation Estimates. *Remote Sensing*, 11, 1345. https://doi.org/10.3390/rs11111345.

Mastrantonas, N., Bhattacharya, B., Shibuo, Y., Rasmy, M., Espinoza-Dávalos, G., Solomatine, D., 2019. Evaluating the Benefits of Merging Near-Real-Time Satellite Precipitation Products: A Case Study in the Kinu Basin Region, Japan. *Journal of Hydrometeorology*. https://doi.org/10.1175/JHM-D-18-0190.1.

Meema, T., Wattanasetpong, J., Wichakul, S., 2025. Integrating machine learning and zoning-based techniques for bias correction in gridded precipitation data to improve hydrological estimation in the data-scarce region. *Journal of Hydrology*, 646, 132356. https://doi.org/10.1016/j.jhydrol.2024.132356.

Nie, S., Luo, Y., Wu, T., Shi, X., Wang, Z., 2015. A merging scheme for constructing daily precipitation analyses based on objective bias-correction and error estimation techniques. *Journal of Geophysical Research*, 120, 8671–8692. https://doi.org/10.1002/2015JD023347.

Pratama, A., Buono, A., Hidayat, R., Harsa, H., 2018. Bias correction of daily satellite precipitation data using genetic algorithm. *IOP Conference Series: Earth and Environmental Science*, 149, 012071.

Seo, G.-Y., Ahn, J.-B., 2023. Comparison of Bias Correction Methods for Summertime Daily Rainfall in South Korea Using Quantile Mapping and Machine Learning Model. *Atmosphere*, 14, 1057. https://doi.org/10.3390/atmos14071057.

Wehbe, Y., Temimi, M., Adler, R., 2020. Enhancing Precipitation Estimates Through the Fusion of Weather Radar, Satellite Retrievals, and Surface Parameters. *Remote Sensing*, 12, 1342. https://doi.org/10.3390/rs12081342.

Xiao, S., Zou, L., Xia, J., Yang, Z., Yao, T., 2022. Bias correction framework for satellite precipitation products using a rain/no rain discriminative model. *Science of The Total Environment*, 818, 151679. https://doi.org/10.1016/j.scitotenv.2021.151679.

Yan, X., Chen, H., Tian, B., Sheng, S., Wang, J., Kim, J.-S., 2021. A Downscaling–Merging Scheme for Improving Daily Spatial Precipitation Estimates Based on Random Forest and Cokriging. *Remote Sensing*, 13, 2040. https://doi.org/10.3390/rs13112040.

Yang, Z., Hsu, K., Sorooshian, S., Xu, X., Braithwaite, D., Verbist, K., 2016. Bias adjustment of satellite-based precipitation estimation using gauge observations: A case study in Chile. *Journal of Geophysical Research: Atmospheres*, 121, 3790–3806. https://doi.org/10.1002/2015JD024540.

Yoshikane, T., Yoshimura, K., 2022. A bias correction method for precipitation through recognizing mesoscale precipitation systems corresponding to weather conditions. *PLOS Water*, 1, e0000016. https://doi.org/10.1371/journal.pwat.0000016.

Zarei, M., Najarchi, M., Mastouri, R., 2021. Bias correction of global ensemble precipitation forecasts by Random Forest method. *Earth Science Informatics*, 14, 677–689. https://doi.org/10.1007/s12145-021-00577-7.

Zhang, L., Li, X., Zheng, D., Zhang, K., Ma, Q., Zhao, Y., Ge, Y., 2021. Merging multiple satellite-based precipitation products and gauge observations using a novel double machine learning approach. *Journal of Hydrology*, 594, 125969. https://doi.org/10.1016/j.jhydrol.2021.125969.

Zhou, L., Koike, T., Takeuchi, K., Rasmy, M., Onuma, K., Ito, H., Selvarajah, H., Liu, L., Li, X., Ao, T., 2022. A study on availability of ground observations and its impacts on bias correction of satellite precipitation products and hydrologic simulation efficiency. *Journal of Hydrology*, 610, 127595. https://doi.org/10.1016/j.jhydrol.2022.127595.